A Variance Distribution Model of Surface EMG Signals Based on Inverse Gamma Distribution

Hideaki Hayashi, *Member, IEEE,* Akira Furui, Junichi Imagi, Yuichi Kurita, *Member, IEEE,* and Toshio Tsuji, *Member, IEEE*

著者に古居追加

***Abstract*—This paper describes the formulation of a surface electromyogram (EMG) model capable of representing the variance distribution of EMG signals. In the model, EMG signals are handled based on a Gaussian white noise process with a mean of zero for each variance value. EMG signal variance is taken as a random variable that follows inverse gamma distribution, allowing the representation of noise superimposed onto this variance. Variance distribution is estimated using rectified and smoothed EMG signals, thereby allowing the determination of distribution parameters at low computational cost. A simulation experiment was performed to evaluate the accuracy of distribution estimation using artificially generated EMG signals, with results demonstrating that the proposed model's accuracy is higher than that of maximum likelihood-based estimation. Analysis of variance distribution using real EMG data also suggested a relationship between variance distribution and signal-dependent noise.**

***Index Terms*—Electromyogram (EMG), variance distribution, smoothed and rectified signals, signal-dependent noise.**

I. Introduction

SURFACE electromyogram (EMG) signals, which can be measured from the skin surface, reflect muscular activity. Examples of their application in a wide range of fields, such as rehabilitation, prosthesis control, and motion analysis [1]–[11], include work by Song *et al.* [1], who conducted myoelectrically controlled upper-limb training for post-stroke patients and showed resulting improvement of upper-limb function. Fukuda *et al.* [4] and Shenoy *et al.* [5] also achieved multifunctional prosthesis control using EMG signals measured from multiple electrodes.

In view of the need for appropriate feature extraction in the achievement of these applications, various quantitative evaluation methods for EMG signals have been proposed [12]–[22]. By way of example, frequency domain features such as autoregressive coefficients (AR) [18] and median frequencies (MF) [19] are often used, and their validity for EMG classification has also been demonstrated [9], [10]. However, computation to extract frequency features is time-consuming, and is not always suitable for applications such as prosthesis control where real-time operation is required. In contrast, amplitude features are widely used because of their relatively low computation cost [1]–[8], [11]. The most common methods include rectifying and smoothing processing [12] as seen in the operation of the MyoBock (Otto Bock HealthCare) [11], which is currently the most popular myoelectric hand. This method is useful in practice because the processed signals are composed of low-frequency components, and the sampling frequency can therefore be reduced to some extent. In the processing method, the relationship between the processed EMG signal and the corresponding muscle force has been elucidated experimentally [12] but not theoretically.

Meanwhile, Hogan and Mann modeled the relationship between muscle force and raw EMG signals based on Gaussian distribution with a zero mean [15], [16], and hence the muscle force estimation problem can be attributed to the variance estimation problem in raw EMG signals. In the model, however, noise superimposed onto the variance of EMG signals depending on muscle force [23]–[25] cannot be considered because the model estimates variance using the maximum likelihood method under the assumption that variance is constant. The model also has another drawback in that numerous data are required for accurate estimation because the data used in the model are raw EMG signals with a high-frequency component.

This paper proposes a surface EMG model that involves variance distribution in consideration of force-dependent noise based on rectified and smoothed signals and inverse gamma distribution. The model estimates variance distribution with EMG variance taken as a random variable, thereby allowing the representation of noise superimposed onto variance depending on muscle force. EMG variance distribution can also be estimated in a small number of samples using rectified and smoothed signals.

The rest of this paper is organized as follows: Section II outlines the structure of the proposed model and the parameter estimation method, Section III details the experimental setup for model verification using artificial data and EMG data, Section IV outlines the results, Section V provides related discussion, and Section VI presents the conclusion.

II. Surface EMG Model

A. Model Structure

Fig. 1 gives an overview of the proposed model, which expresses an EMG signal x based on a process involving white Gaussian noise W passed through a shaping filter H and a random variable σ^2, which is the variance of EMG signals with distribution determined by $\bar{\sigma}^2$ and noise ε depending on the exerted muscle force f.

H. Hayashi, Y. Kurita, and T. Tsuji are with Institute of Engineering, Hiroshima University, Higashi-hiroshima, 739-8527 Japan (e-mail: hayashi@bsys.hiroshima-u.ac.jp).

A. Furui and J. Imagi are with Graduate School of Engineering, Hiroshima University, Higashi-hiroshima, 739-8527 Japan.

Manuscript received April 19, 2005; revised December 27, 2012.

モデル部と推定部を明示的に分割

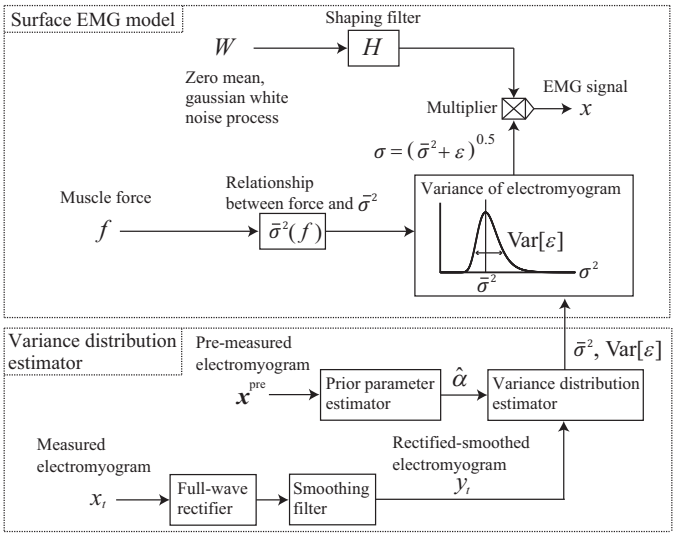

Fig. 1. Overview of the proposed model. The model expresses an EMG signal x based on a process involving white Gaussian noise W passed through a shaping filter H and a random variable σ^2, which is the variance of EMG signal whose distribution is determined by $\bar{\sigma}^2$ and noise ε depending on muscle force f.

First, the relationship between f and $\bar{\sigma}$ can be expressed as follows [15], [16]:

$$\bar{\sigma} = kf^a, \tag{1}$$

where k and a are constants that can be experimentally estimated [15], [16]. σ^2 is then represented by the sum of $\bar{\sigma}^2$ and noise ε.

$$\sigma^2 = \bar{\sigma}^2 + \varepsilon, \tag{2}$$

where ε is a random variable with a zero mean. The mean $E[\sigma^2]$ and the variance $Var[\sigma^2]$ of σ^2 are therefore calculated as

Gaussianになるのはある分散値で条件づけられた筋電分布

$$E[\bar{\sigma}^2] + E[\varepsilon] = \bar{\sigma}^2, \tag{3}$$
$$E[(\sigma^2 - \bar{\sigma}^2)^2] = Var[\varepsilon]. \tag{4}$$

Because x is expressed as the multiplication of σ and white Gaussian noise W passed through H, the conditional distribution of x given σ^2 is Gaussian distribution with a mean of zero and a variance of σ^2:

$$P(x|\sigma^2) = \frac{1}{\sqrt{2\pi\sigma^2}} \exp\left[-\frac{x^2}{2\sigma^2}\right]. \tag{5}$$

B. Estimation of Variance Distribution

This subsection outlines estimation to determine the distribution of σ^2. Considering that $\sigma^2 > 0$, the inverse gamma distribution $\mathrm{IG}(\alpha, \beta)$ (also known as a conjugate prior for Gaussian distribution) is chosen as the distribution $P(\sigma^2)$.

$$P(\sigma^2) = \mathrm{IG}(\sigma^2; \alpha, \beta) = \frac{\beta^\alpha}{\Gamma(\alpha)} (\sigma^2)^{-\alpha-1} e^{-\frac{\beta}{\sigma^2}}, \tag{6}$$

where α and β are parameters that determine inverse gamma distribution and are referred to as the shape parameter and the scale parameter, respectively [26]. Given N samples of EMG signals $\boldsymbol{x} = \{x_n\}_{n=1}^N$ as observations recorded with a constant muscle force, the parameters $[\hat{\alpha}, \hat{\beta}]$ where observations are most likely to occur are estimated by maximizing the marginal likelihood of $\boldsymbol{x}$, $P(\boldsymbol{x}; \alpha, \beta)$.

生筋電を用いた周辺尤度最大化に基づく分散分布推定法の追加
ベイズの定理に基づく各時刻の分散値の事後分布推定を削除

$$[\hat{\alpha}, \hat{\beta}] = \arg\max_{\alpha,\beta} P(\boldsymbol{x}; \alpha, \beta) \tag{7}$$

Assuming that values of $\{x_n\}_{n=1}^N$ are independent, the marginal likelihood is expanded as follows:

$$\begin{aligned} & P(\boldsymbol{x}; \alpha, \beta) \\ &= \prod_{n=1}^N P(x_n; \alpha, \beta) \\ &= \prod_{n=1}^N \int_{\sigma_n^2} P(x_n|\sigma_n) P(\sigma_n; \alpha, \beta) d\sigma_n^2 \\ &= \prod_{n=1}^N \int_{\sigma_n^2} \frac{1}{\sqrt{2\pi\sigma_n^2}} e^{-\frac{x_n^2}{2\sigma_n^2}} \frac{\beta^\alpha}{\Gamma(\alpha)} (\sigma_n^2)^{-\alpha-1} e^{-\frac{\beta}{\sigma_n^2}} d\sigma_n^2 \\ &= \prod_{n=1}^N \frac{\beta^\alpha \Gamma(\alpha + \frac{1}{2})}{\sqrt{2\pi}\Gamma(\alpha) \left(\beta + \frac{x_n^2}{2}\right)^{\alpha+\frac{1}{2}}}. \end{aligned} \tag{8}$$

The details of calculation for optimization are presented in the Appendix. Using the estimated variance distribution parameters $[\hat{\alpha}, \hat{\beta}]$, the mean $E[\sigma^2]$ and the variance $Var[\sigma^2]$ of variance distribution are then given as follows:

$$E[\sigma^2] = \frac{\hat{\beta}}{\hat{\alpha} - 1}, \tag{9}$$
$$Var[\sigma^2] = \frac{\hat{\beta}^2}{(\hat{\alpha} - 1)^2(\hat{\alpha} - 2)}. \tag{10}$$

From (3) and (4), $E[\sigma^2]$ and $Var[\sigma^2]$ correspond to the estimated values of $\bar{\sigma}^2$ and $Var[\varepsilon]$, respectively. Using the above procedure, variance distribution can be estimated from recorded EMG signals.

However, this estimation procedure requires repetitive calculation during nonlinear optimization, meaning that variance distribution cannot be calculated in real time. The next subsection outlines the method used to approximate variance distribution using rectified and smoothed EMG signals for the achievement of real-time estimation.

C. Estimation Using Rectified and Smoothed EMG Signals

We first consider the estimation of $\bar{\sigma}$. Given an EMG signal stream x_t $(t = 1, \cdots, T)$, y_t is first calculated by rectifying and smoothing x_t using an N-order low pass filter:

$$\begin{aligned} y_t = {} & a_0 y_{t-1} + a_1 y_{t-2} + \cdots + a_{N-1} y_{t-N} \\ & + b_0|x_t| + b_1|x_{t-1}| + \cdots + b_N|x_{t-N}|, \end{aligned} \tag{11}$$

where $a_0, a_1, \cdots, a_{N-1}$ and $b_0, b_1, \cdots, b_N$ are filter coefficients. The expectation of y_t is then derived as follows:

$$\begin{aligned} E[y_t] = {} & a_0 E[y_{t-1}] + a_1 E[y_{t-2}] + \cdots + a_{N-1} E[y_{t-N}] \\ & + b_0 E[|x_t|] + b_1 E[|x_{t-1}|] + \cdots + b_N E[|x_{t-N}|]. \end{aligned} \tag{12}$$

$E[|x_t|]$ can be calculated with the following formula because x_t obeys the distribution in (5):

$$\begin{aligned} E\left[|x_t|\right] &= \int_{-\infty}^{\infty} |x_t| \frac{1}{\sqrt{2\pi\sigma_t^2}} \exp\left[-\frac{x_t^2}{2\sigma_t^2}\right] dx_t \\ &= \sqrt{\frac{2\sigma_t^2}{\pi}} \\ &= \sqrt{\frac{2}{\pi}\left(\bar{\sigma}^2 + \varepsilon_t\right)} \\ &\simeq \sqrt{\frac{2}{\pi}}\left(\bar{\sigma} + \frac{1}{2}\frac{\varepsilon_t}{\bar{\sigma}}\right). \end{aligned} \tag{13}$$

Assuming that y_t is temporally stable, (12) and (13) give the following equation:

$$\frac{1-\sum_{i=1}^{N-1} a_i}{\sum_{i=0}^{N} b_i}\sqrt{\frac{\pi}{2}} E[y_t] = \bar{\sigma} + \frac{1}{2\bar{\sigma}} \frac{\sum_{i=0}^{N} b_i \varepsilon_{t-i}}{\sum_{i=0}^{N} b_i}. \tag{14}$$

In (14), the second term on the right-hand side is sufficiently smaller than the first term to be ignored because it has a weighted average of ε_t ($\ll \bar{\sigma}$) based on b_i (> 0) and its expectation is 0. Using (14), $\bar{\sigma}^2$ can therefore be estimated as follows:

$$\bar{\sigma}^2 = \left(\frac{1-\sum_{i=1}^{N} a_i}{\sum_{i=0}^{N} b_i}\right)^2 \frac{\pi}{2} E\left[y_t\right]^2, \tag{15}$$

where the fractional term on the right-hand side corresponds to the reciprocal of the filter gain. Because of the assumption that y_t is temporally stable, $E\left[y_t\right]$ can be substituted by a moving average of the past L samples (L is the width of the time window). Note that the raw EMG signal x_t is not required

整流平滑化法による分散分布の分散推定式を明記

$Var[\varepsilon]$ can then be calculated from $\bar{\sigma}^2$ using the relationship between (9) and (10) as

$$Var[\varepsilon] = \frac{(\bar{\sigma}^2)^2}{(\hat{\alpha}-2)}. \tag{16}$$

In this calculation, $\hat{\alpha}$ is fixed and is estimated prior to the measurement of x_t using a pre-measured EMG data set $\boldsymbol{x}^{\mathrm{pre}}$ based on (7) and (8).

III. Experiments

A. Simulation

To evaluate the accuracy of the proposed model for the estimation of variance distribution, simulation experiments were conducted. Artificially generated EMG signals with variance featuring noise superimposed were first generated in line with the following procedures:

(1) A discrete series $\{\sigma_t^2; t = 1, \cdots, T\}$ was generated using random numbers that obey IG(α_0, β_0).
(2) A normal random number that obeys $\mathcal{N}(0, \sigma_t^2)$ was generated for each t and defined as $\{x_t\}$.
(3) $\{x_t\}$ values were regarded as EMG signals measured at a sampling frequency of F_{s} Hz.

True values for the average of variance and the variance of variance were then given as

$$\bar{\sigma}_0^2 = \frac{\beta_0}{\alpha_0 - 1}, \tag{17}$$

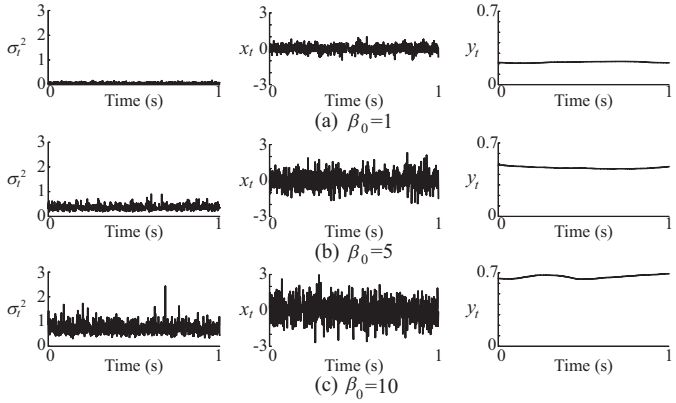

Fig. 2. Examples of σ_t^2, x_t and y_t. σ_t^2 is generated as a random number that obeys IG(α_0, β_0), x_t is a normal random number obeying $\mathcal{N}(0, \sigma_t^2)$ at each t, and y_t is the rectified and smoothed signal of x_t. The data generation parameter β_0 is set as (a) $\beta_0 = 1$, (b) $\beta_0 = 5$, and (c) $\beta_0 = 10$.

$$Var[\varepsilon_0] = \frac{\beta_0^2}{(\alpha_0-1)^2(\alpha_0-2)}. \tag{18}$$

Fig. 2 shows examples of the time-series waveforms of σ_t^2, x_t and y_t, where the data generation parameter β_0 is set as (a) $\beta_0 = 1$, (b) $\beta_0 = 5$, and (c) $\beta_0 = 10$. The vertical and horizontal axes indicate the value of each signal and time, respectively. Accuracy in distribution estimation was verified by comparing true values with $\bar{\sigma}^2$ and $Var[\varepsilon]$ estimated using the proposed model. As an index of accuracy, the error rate was defined as $|\text{true value} - \text{estimated value}|/(\text{true value}) \times 100$.

To verify the validity of approximation using rectified and smoothed signals in the proposed method, the accuracy of variance distribution estimation was compared with that of marginal likelihood maximization-based estimation ((7)–(10)). In this experiment, the T and F_{s} values used for data generation were set as 100 000 ms and 1000 Hz, respectively, and a total of 100 000 samples were therefore used in both estimation methods. The initial values of α and β for marginal likelihood maximization-based estimation were set using uniform random numbers in the range of $(0, 10)$. Average percentage errors were calculated by changing the true values 60 times ($\alpha_0 = 10, 15, 20$, $\beta_0 = 0.5, 1, 1.5, \cdots, 10$), and a second-order Butterworth low-pass filter (cut-off frequency F_{cut}: 1 Hz) was used in smoothing processing.

周辺尤度最大化法（生筋電を用いた推定）と整流平滑化法の精度比較を追加

imum likelihood method with varying window lengths and down-sampling frequency values. In the estimation of $\bar{\sigma}^2$, the last L ms of signals $\{y_t\}$ down-sampled at F_{down} Hz was used, where $\{y_t\}$ represents rectified and smoothed signals of $\{x_t\}$. Percentage errors between $\bar{\sigma}_0^2$ and $\bar{\sigma}^2$ were then calculated with F_{down} varied as 500, 100, 50, 20, and 10 Hz for a fixed value of $L = 1000$ ms, and with L varied as 10 000, 5000, 2000, 1000, 500, 200, 100, 50, and 10 ms for a fixed value of $F_{\mathrm{down}} = 1000$ Hz. The results were also compared with those of maximum likelihood estimators for variance calculated using $\{x_t\}$. In verification of accuracy for the estimation of $Var[\varepsilon]$, percentage errors between $Var[\varepsilon]$ and $Var[\varepsilon_0]$ were calculated with F_{down} varied as 1000 and 50 Hz for

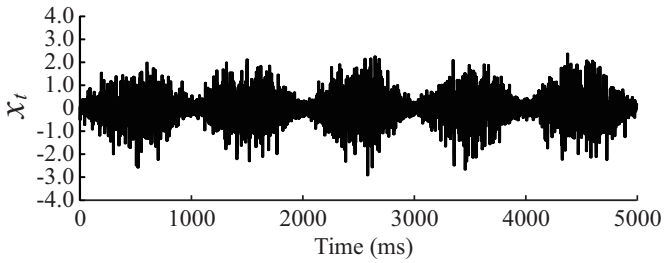

Fig. 3. Sample artificial EMG signals with time-varying force

a fixed value of $L = 1000$ ms, and were then compared with those of variance of variance based on maximum likelihood estimation. This is the variance of K maximum-likelihood variance estimators calculated by dividing L ms of $\{x_t\}$ into K equal parts and estimating the variance for each part. Values of $T = 1000$ and $F_s = 1000$ were set in this experiment, and nd the low-pass filter settings were n.

動的筋力変化時のシミュレーション追加

Finally, variance distribution estimation for artificial EMG signals simulated with changing force was conducted. Signal Generation here followed the procedure described above, but the scale parameter β_0 was changed using the following equation to generate signals with time-varying distribution:

$$\beta_0(t) = \left| \frac{1}{2}(\beta_{\max} - \beta_{\min}) \left\{ \sin\left(\frac{2\pi t}{T_c}\right) + 1 \right\} + \beta_{\min} \right|, \quad (19)$$

where $\beta_{\max}$, $\beta_{\min}$, and T_c are parameters that determine the amplitude and cycle of signals, set as 10, 0.5, and 1000 ms, respectively. Fig. 3 shows an example of artificial EMG signals with simulated changing force. Variance distribution estimation was then conducted using a window length of L ms, with the window shifted for each sample. The residual sum of squares (RSS) defined using the equations below with window lengths L of 1, 5, 10, 20, 50, and 100 ms and cut-off frequencies F_{cut} of 1, 3, 5, 7, 9, 11, and 13 Hz were used to evaluate estimation accuracy.

$$\text{RSS}_{\bar{\sigma}^2} = \sum_{t=1}^{T} \left(\bar{\sigma}^2(t) - \bar{\sigma}_0^2(t)\right)^2, \quad (20)$$

$$\text{RSS}_{Var[\varepsilon]} = \sum_{t=1}^{T} \left(Var[\varepsilon](t) - Var[\varepsilon_0](t)\right)^2, \quad (21)$$

where $\bar{\sigma}_0^2(t)$ and $Var[\varepsilon_0](t)$ are true values for variance distribution at t calculated using (17) and (18), and $\bar{\sigma}^2(t)$ and $Var[\varepsilon](t)$ are estimated values calculated using the proposed method. Ten trials were conducted for each combination of L and F_{cut} by regenerating artificial EMG signals for calculation of average RSS values. The remaining parameters were set as $T = 5000$ ms, $F_s = 1000$ Hz, and $\alpha_0 = 15$.

B. EMG Analysis

To determine the effectiveness of the proposed model for real biological data, estimation experiments on EMG variance distribution $P(\sigma^2)$ were conducted. For EMG signal recording, ten right-handed subjects (average age: 22.6 ± 0.8) were

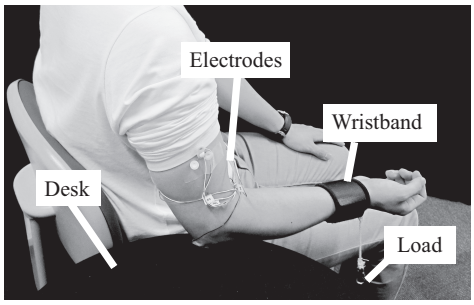

Fig. 4. EMG recording set-up. The subjects were seated with the right upper arm pointing downward, the right forearm bent forward to the horizontal and the palm turned upward. EMG signals were recorded from a pair of electrodes attached to the biceps brachii while the subjects were weighted with a load on the right wrist and maintained position with the elbow on a desk.

seated with the right upper arm pointing downward, the right lower arm bent forward to the horizontal and the palm turned upward (Fig. 4). EMG signals were recorded from a pair of Ag/AgCl electrodes placed 2 cm apart on the biceps brachii with a sampling frequency of 1000 Hz while the subjects were weighted with a load hanging vertically from a wristband on the right wrist. The subjects were instructed to keep the elbow at a right-angle for 10 seconds with the elbow on a desk (Fig. 4). The load weight was varied at 500, 1000, 1500, and 2000 g, and five trials were conducted for each load weight. A multi-telemeter system (NIHON KOHDEN, WEB-5000; high-frequency cutoff: 100 Hz; low-frequency cutoff: 5.3 Hz) was used for measurement. All subjects were told the aim of the experiment and gave informed consent prior to the trials.

The latter five-second part of the ten seconds of recorded data was used for EMG analysis. The muscle force f of the biceps brachii was also calculated using the following equation assuming that the ratio of forearm/hand weight to body weight was 0.022 [27], the ratio of the length from the elbow to the center of gravity to the length of the forearm/hand (defined as the length from the elbow axis to the ulnar styloid) was 0.682 [27], and the moment arm length of the biceps brachii to the rotational center of the elbow was 0.03 m [28].

$$f = \frac{0.022M \times 0.682L_f + W \times L_f}{0.03}, \quad (22)$$

where M is the body weight, W is the load weight, and L_f is the length from the elbow axis to the ulnar styloid. The EMG variance distribution was then calculated for each muscle force level. The parameter $\hat{\alpha}$ for the proposed model was estimated using marginal likelihood maximization with single-trial EMG signals recorded in advance under a 2000 g load.

Regression analysis was also conducted to establish the relationship between muscle force and estimated variance distribution statistics. To remove the influence of individual differences (e.g., skin-electrode impedance), estimation statistics ($\bar{\sigma}^2$ and $Var[\varepsilon]$) and muscle force were normalized by their standard deviations for each subject before regression analysis was performed. Based on the assumption that the relationship between muscle force f and $\bar{\sigma}^2$ obeys the power law (equation (1)), the log-linearized power model solved for $\ln(f)$, $\ln(f) = \frac{1}{a}\ln(\bar{\sigma}^2) - \frac{1}{a}\ln(k)$ was fitted by performing linear regression analysis on logarithmic values. This analysis

筋力と分散分布パラメータの回帰分析を追加

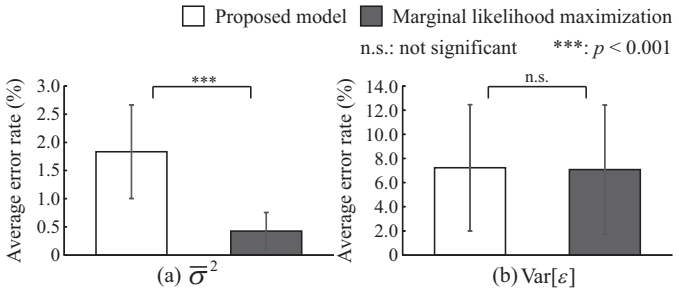

Fig. 5. Average error rates in estimation of $\bar{\sigma}$ and $Var[\varepsilon]$ for the proposed model and marginal likelihood maximization. Error bars represent standard deviations for all trials.

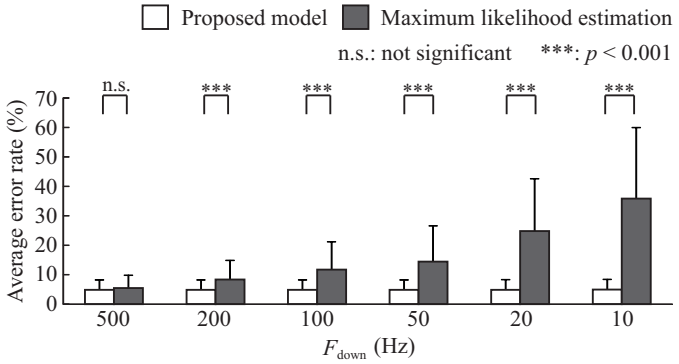

Fig. 6. Average error rates in estimation of $\bar{\sigma}$ for each down-sampling frequency F_{down}. Error bars represent standard deviations for all trials.

was also performed on the relationship between variance of variance $Var[\varepsilon]$ and muscle force. Variance distribution statistics were also calculated on the basis of maximum likelihood estimation as in the simulation experiment. This regression analysis was conducted for full samples ($T = 5000$ and $F_{\mathrm{down}} = 1000$) and small samples ($T = 100$ and $F_{\mathrm{down}} = 100$).

IV. Results

Fig. 5 shows average error rates in estimation of $\bar{\sigma}$ and $Var[\varepsilon]$ for the proposed model and marginal likelihood maximization. The results of paired t-test are also given.

Fig. 6 shows accuracy in the estimation of $\bar{\sigma}^2$ for each values of F_{down} and comparison with maximum likelihood estimation. Significant differences were observed based on t-test when F_{down} was 200 or less. Fig. 7 shows the results for each value of L. Significant differences were observed based on t-test when L was 10 000, 5000, and 200 or less. Fig. 8 shows accuracy in the estimation of $Var[\varepsilon]$. Significant differences were observed between the outcomes of the proposed model and the maximum likelihood method based on the Holm multiple comparison test.

Fig. 9 shows sample variance distribution estimation results for artificial EMG signals with time-varying force. For each combination of parameters, the upper and lower panels show the results of estimation to determine the mean of variance distribution $\bar{\sigma}$ and the variance of variance distribution $Var[\varepsilon]$, respectively. Each graph illustrates a single signal period. Figs. 10 (a) and (b) show average RSS values of $\bar{\sigma}$ and $Var[\varepsilon]$,

L > 1000の結果を追加

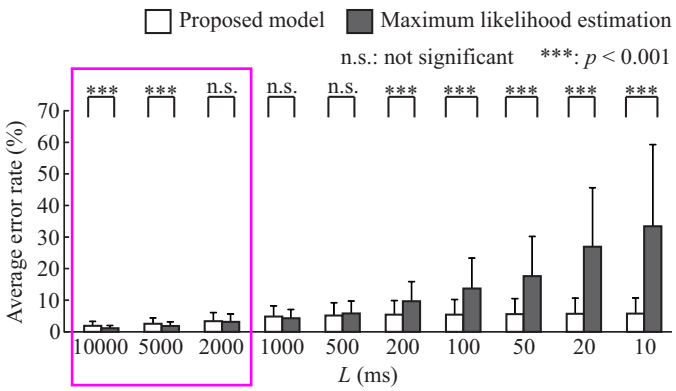

Fig. 7. Average error rates in estimation of $\bar{\sigma}$ for each window width L. Error bars represent standard deviations for all trials.

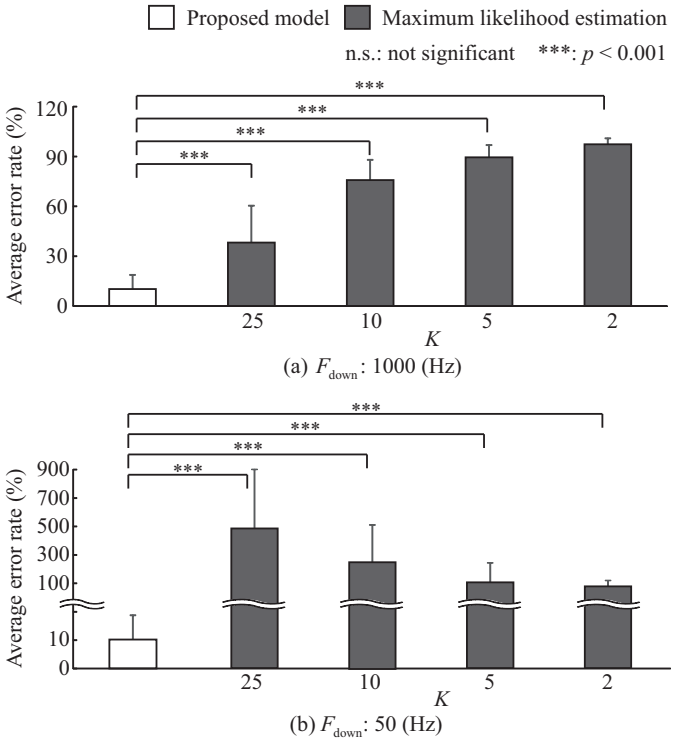

Fig. 8. Average error rates in estimation of $Var[\varepsilon]$ for each down-sampling frequency F_{down} and the number of divisions K. Error bars represent standard deviations for all trials. Vertical axis scale from 20 to 100 is omitted in (b).

respectively, for signals with time-varying force. The results for $F_{\mathrm{cut}} = 1.0$ are omitted due to the excessive nature of their RSS values.

Fig. 11 shows examples of raw EMG signals and rectified and smoothed signals for different load weights of (a) 500 g, (b) 1000 g, (c) 1500 g, and (d) 2000 g. The panels on the left show raw EMG signals, and those on the right show rectified and smoothed signals. Fig. 12 shows the variance distributions $P(\sigma^2)$ for Sub. A in a trial, with the distributions of all load weights shown overlapping. Fig. 13 summarizes the mean of variance $\bar{\sigma}$ and the variance of variance $Var[\varepsilon]$ for Sub. A in all trials for each muscle force, and shows statistical test results based on the Steel-Dwass method. Significant increases in

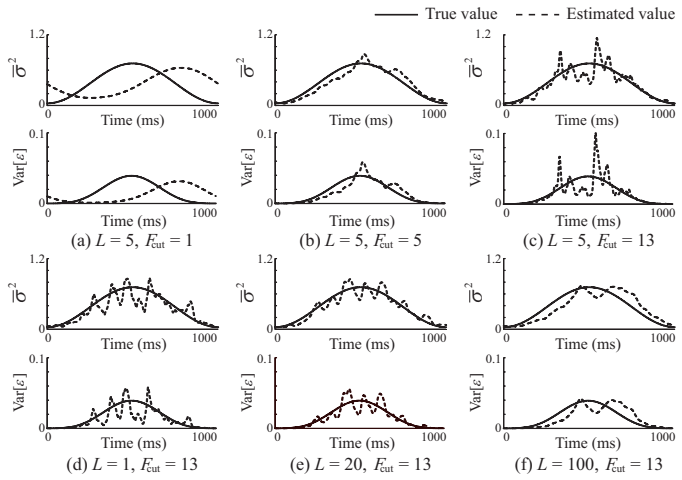

Fig. 9. Sample variance distribution estimation results for artificial EMG signals with time-varying force for certain combinations of parameters (one cycle)

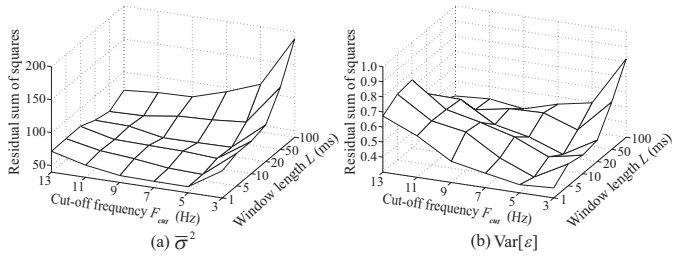

Fig. 10. Average RSS values for estimation of variance distribution for signals with time-varying force. The values for $F_{\mathrm{cut}} = 1.0$ are omitted due to the excessive nature of their RSS values.

the mean of variance and variance of variance with increased muscle force are seen in eight of the ten subjects (significance level: 5 %). In regression analysis regarding the relationships between muscle force f and $\bar{\sigma}$ and between f and $Var[\varepsilon]$, significant regression relationships were observed in all cases. The coefficient of determination (R^2) for the regression $\ln(f)$ on $\ln(\bar{\sigma})$ and $\ln(f)$ on $\ln(Var[\varepsilon])$ in the case of full samples ($T = 5000$ and $F_{\mathrm{down}} = 1000$) were 0.37 and 0.40 for the proposed model and 0.35 and 0.30 for maximum likelihood estimation, respectively. The regression analysis results in the case of small samples ($T = 100$ and $F_{\mathrm{down}} = 100$) are summarized in Fig. 14, which also shows the regression equations, the coefficient of determination (R^2), F values, and p values for the F test.

V. Discussion

In Fig. 5, the average error rate of $\bar{\sigma}^2$ for the proposed model is significantly larger than that for marginal likelihood maximization. However, the error value itself is less than 2 %, indicating that the approximation employed in the proposed model is appropriate in consideration of the fact that it enables real-time estimation. Meanwhile, the average error rates of $Var[\varepsilon]$ for both methods are around 7 %, and are larger than those of $\bar{\sigma}^2$. This indicates that variance of variance is more difficult to estimate than the mean of variance.

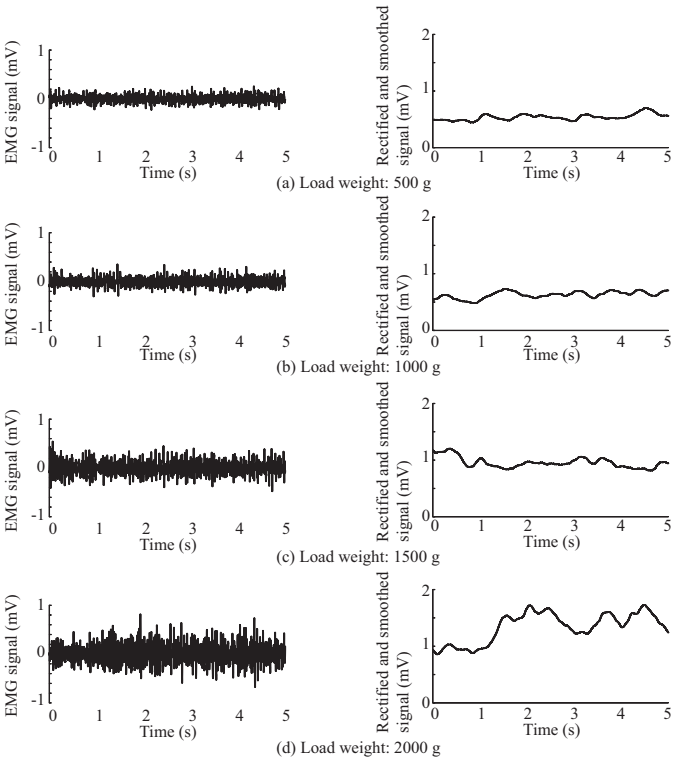

Fig. 11. Examples of EMG signals and rectified/smoothed signals (Subject A). The panels on the left show EMG signals, and those on the right show rectified/smoothed signals. A second-order Butterworth low-pass filter (cut-off frequency F_{cut}: 1 Hz) was used in smoothing processing.

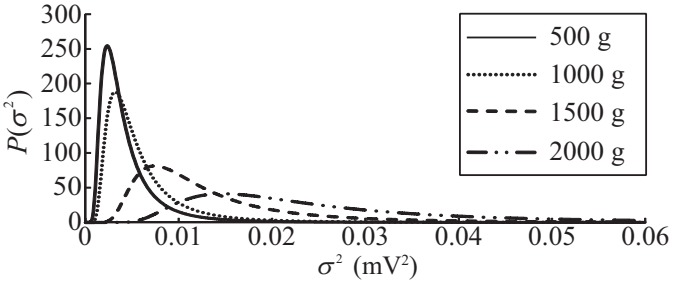

Fig. 12. Example of the variance distribution $P(\sigma^2)$ for Sub. A. The distributions of all load weights are shown overlapping.

Fig. 6 shows equally high accuracy for the proposed model and the maximum likelihood method when the sampling frequency F_{down} was high. The accuracy of the maximum likelihood method, however, decreased as F_{down} decreased, whereas the proposed model maintained high accuracy with an error rate of less than 5 %. In Fig. 7, both methods show high accuracy at $L = 10\ 000$ ms with an error rate of less than 2 %, whereas maximum likelihood estimation was slightly better than with the proposed model. Although the accuracy of both methods decreased with lower values of L, the average error rate for the proposed model was about 5 % even at $L = 10$ ms, and was significantly lower than that of the maximum likelihood method. These results indicate that the proposed model can be used to estimate $\bar{\sigma}^2$ with a small number of samples. This is because the maximum likelihood method is sensitive to outliers and bias in data measurement in principle,

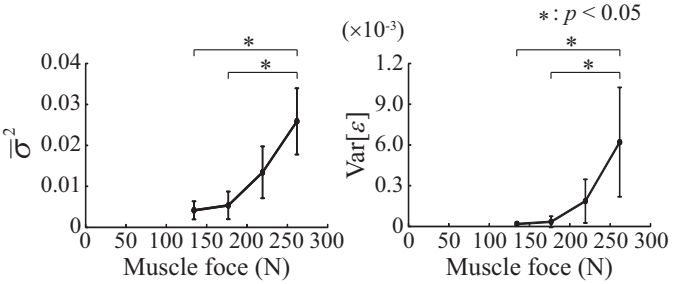

Fig. 13. Mean of variance $\bar{\sigma}$ (left) and variance of variance $Var[\varepsilon]$ (right) for each muscle force (Sub. A). Error bars represent standard deviations for

筋力と分散分布パラメータの回帰分析を追加

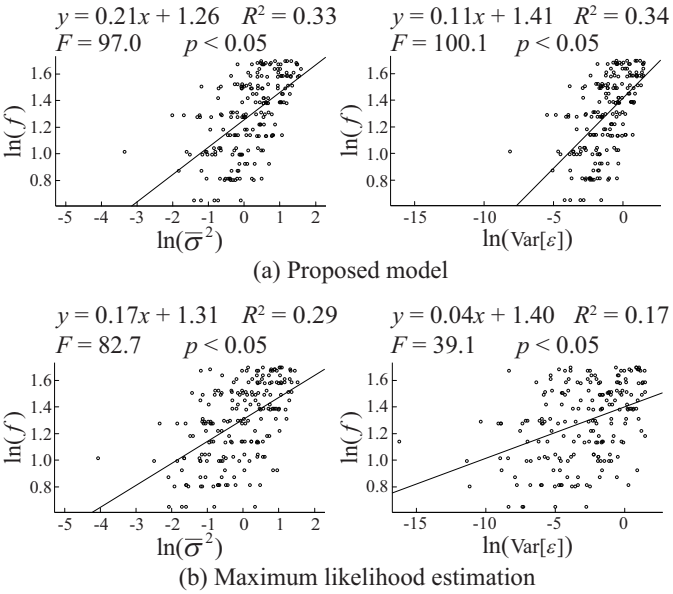

Fig. 14. Results of regression analysis to determine the relationships between muscle force f and $\bar{\sigma}$, and between f and $Var[\varepsilon]$ for (a) the proposed method and (b) maximum likelihood estimation. The figure also shows the regression equations, the coefficient of determination R^2, F values, and p values for the F test.

whereas the low-pass filter involved in the proposed model smooths data and mitigates such adverse influences.

Fig. 8 shows that the average error rates in estimation of $Var[\varepsilon]$ for the proposed model were significantly lower than those for the maximum likelihood. This is because the maximum likelihood method involves the assumption that variance is constant in each division, and cannot sufficiently express the noise superimposed onto variance independently at each time. In contrast, the proposed model involves the assumption that variance is independent at each time, and estimates the distribution of their population. Accordingly, the variance of variance can be estimated with an average error rate of less than about 10 %.

In Figs. 9 (a)–(c), the variation of estimated values grows as the cut-off frequency $F_{\rm cut}$ increases, whereas delays occur in the low cut-off frequency. Delays are also observed with greater window lengths, although variations in estimated values become smaller as the window length L increases (Figs. 9 (d)–(f)). The trade-off between the stability of estimation and followability to time variation can be controlled using the parameters $F_{\rm cut}$ and L. As shown in Fig. 10, RSS values were the smallest at $F_{\rm cut} = 5$ and $L = 5$ in this experiment. These results show that the proposed model can be used to track time-varying signals if the parameters $F_{\rm cut}$ and L are appropriately set.

In Fig. 12, the variance distributions $P(\sigma^2)$ shift to the right and spread horizontally as the load increases. Accordingly, the mean and variance tend to increase with greater loads. Fig. 13 indicates that the relationship between the variance mean $\bar{\sigma}^2$ and muscle force can be expressed by (1) because of their monotonic increasing relationship. The regression analysis results shown in Fig. 14 indicate that the overall coefficients of determination tended to be low because the variance of muscle force was large. However, both $\bar{\sigma}^2$ and $Var[\varepsilon]$ estimated using the proposed model showed better fits than those estimated based on maximum likelihood estimation even with small samples. These results indicate that mean of variance $\bar{\sigma}^2$ and variance of variance $Var[\varepsilon]$ estimated using the proposed model both have potential in the estimation of muscle force f.

The proposed model involves the assumption that EMG variance becomes a random variable via superimposition of noise. In the estimation procedure, it is also assumed that variance follows inverse gamma distribution with a fixed shape parameter α. These assumptions bring two properties associated with previous studies. One is the relationship to signal-dependent noise. Harris and Wolpert assumed that neural commands have signal-dependent noise whose standard deviation increases linearly with the absolute value of the neural control signal [23]. Jones *et al.* experimentally showed that the standard deviation of force is proportional to the mean force during isometric contraction [24]. From the relationship between the mean of variance and variance of variance formulated in (16), the proposed model implicitly derives that the standard deviation of σ^2 is proportional to the mean of σ^2, and demonstrates that a similar relationship found in terms of force in [24] can also be established in EMG variance. The other is the property of marginal distribution for EMG signals. Hogan and Mann [15] modeled EMG signals as a random process whose distribution is Gaussian with a zero mean, but this idea does not meet general consensus. Clancy and Hogan [17] experimentally observed that the probability density of EMG falls between Gaussian and Laplacian densities. Nazarpour *et al.* also found that EMG density exhibits kurtosis at low contraction levels. Although the proposed model involves the assumption of Gaussian as EMG distribution for each variance value $P(x|\sigma^2)$, the marginal distribution of EMG $P(x)$ is no longer Gaussian due to noise superimposed onto variance, and is calculated using the similar procedure of (8).

$$P(x) = \frac{\beta^{\alpha}\Gamma(\alpha+\frac{1}{2})}{\sqrt{2\pi}\Gamma(\alpha)\left(\beta+\frac{x^2}{2}\right)^{\alpha+\frac{1}{2}}} \tag{23}$$

This distribution is equivalent to Student's t-distribution with a different parameterization as $\nu = 2\alpha$ and $s^2 = \beta/\alpha$, where ν is the number of degrees of freedom and s is the scale parameter. As the t-distribution exhibits a kurtosis

この研究で得られた知見と従来研究を比較した際の考察を追加

of $\frac{6}{\nu-4}$ for $\nu > 4$ (i.e., $\frac{3}{\alpha-2}$ for $\alpha > 2$), the proposed model consequently represents the marginal distribution of EMG using the t-distribution with fixed kurtosis and changing variance depending on muscle force.

VI. Conclusion

This paper proposed a surface EMG signal model that incorporates variance distribution in consideration of force-dependent noise. The proposed model is used to determine the distribution of variance in EMG signals based on rectified and smoothed signals, thereby allowing the expression of noise superimposed onto variance depending on force.

Simulation using artificial EMG signals revealed that the proposed method can be used to estimate the mean of variance and variance of variance using a smaller number of samples with a higher level of accuracy than with maximum likelihood estimation. Simulation results also showed that the proposed model can be used to track time-varying signals if the parameters are appropriately set. Estimation of variance distribution in EMG signals recorded from ten subjects also indicated that the mean of variance and variance of variance increased with force, which corresponds to the previously reported trend of muscle force variance [24]. Regression analysis indicated that the mean of variance and variance of variance estimated using the proposed model both have potential as estimators of muscle force.

Limitations of this study include the absence of evaluation to determine the influence of fatigue and posture on EMG variance distribution and the need for practical application of the proposed model. In future research, the authors plan to apply the model to EMG pattern classification and artificial EMG generation.

Appendix
Marginal Likelihood Maximization

As the maximization of $P(\boldsymbol{x};\alpha,\beta)$ is equivalent to the minimization of $-\log P(\boldsymbol{x};\alpha,\beta)$, the evaluation function $J(\alpha,\beta,\boldsymbol{x})$ is then defined for minimization as follows:

$$\begin{aligned} J(\alpha,\beta,\boldsymbol{x}) &= -\log P(\boldsymbol{x};\alpha,\beta) \\ &= -\sum_{n=1}^{N}\left\{-\frac{1}{2}\log(2\pi)+\alpha\log\beta-\log\Gamma(\alpha)\right. \\ &\quad \left.+\log\Gamma\left(\alpha+\frac{1}{2}\right)-\left(\alpha+\frac{1}{2}\right)\log\left(\beta+\frac{x_n^2}{2}\right)\right\} \\ &= \frac{N}{2}\log 2\pi - N\alpha\log\beta + N\log\Gamma(\alpha) \\ &\quad -N\log\Gamma\left(\alpha+\frac{1}{2}\right)+\left(\alpha+\frac{1}{2}\right)\sum_{n=1}^{N}\log\left(\beta+\frac{x_n^2}{2}\right). \end{aligned} \quad (24)$$

α and β are then updated from arbitrary initial values using the steepest descent method as:

$$\begin{bmatrix} \alpha^{(r+1)} \\ \beta^{(r+1)} \end{bmatrix} = \eta \begin{bmatrix} \frac{\partial J(\alpha^{(r)},\beta^{(r)},\boldsymbol{x})}{\partial\alpha} \\ \frac{\partial J(\alpha^{(r)},\beta^{(r)},\boldsymbol{x})}{\partial\beta} \end{bmatrix}, \quad (25)$$

where η is the update rate, and $\frac{\partial J}{\partial\alpha}$ and $\frac{\partial J}{\partial\beta}$ are derived as follows:

$$\begin{aligned} \frac{\partial J}{\partial\alpha} &= -N\log\beta + N\Psi(\alpha) - N\Psi\left(\alpha+\frac{1}{2}\right) \\ &\quad +\sum_{n=1}^{N}\log\left(\beta+\frac{x_n^2}{2}\right), \end{aligned} \quad (26)$$

$$\frac{\partial J}{\partial\beta} = -\frac{N\alpha}{\beta}+\left(\alpha+\frac{1}{2}\right)\sum_{n=1}^{N}\frac{1}{\beta+\frac{x_n^2}{2}}, \quad (27)$$

where $\Psi(\alpha)$ is a digamma function.

References

[1] R. Song et al., "Assistive control system using continuous myoelectric signal in robot-aided arm training for patients after stroke," *IEEE Trans. Neural Syst. Rehabil. Eng.*, vol. 16, no. 4, pp. 371–379, Aug. 2008.

[2] E. Akdogan et al., "The cybernetic rehabilitation aid: Preliminary results for wrist and elbow motions in healthy subjects," *IEEE Trans. Neural Syst. Rehabil. Eng.*, vol. 20, no. 5, pp. 697–707, Sept. 2012.

[3] S. R. Taal and Y. Sankai, "Exoskeletal spine and shoulders for full body exoskeletons in health care," *Advances in Applied Sci. Research*, vol. 2, no. 6, pp. 270–286, 2011.

[4] O. Fukuda et al., "A human-assisting manipulator teleoperated by emg signals and arm motions," *IEEE Trans. Robot. Autom.*, vol. 19, no. 2, pp. 210–222, Apr. 2003.

[5] P. Shenoy et al., "Online electromyographic control of a robotic prosthesis," *IEEE Trans. Biomed. Eng.*, vol. 55, no. 3, pp. 1128–1135, Mar. 2008.

[6] K. T. Yoo et al., "Motion analysis and emg analysis of the pelvis and lower extremity according to the width variation of the base of support," *J. Int. Academy of Physical Therapy Research*, vol. 3, no. 1, pp. 391–396, 2012.

[7] D. R. Moynes et al., "Electromyography and motion analysis of the upper extremity in sports," *Physical therapy*, vol. 66, no. 12, pp. 1905–1911, 1986.

[8] Z. Ju and H. Liu, "Human hand motion analysis with multisensory information," *Trans. Mechatron.*, vol. 19, no. 2, pp. 456–466, 2014.

[9] R. Boostani and M. H. Moradi, "Evaluation of the forearm emg signal features for the control of a prosthetic hand," *Physiological measurement*, vol. 24, no. 2, p. 309, 2003.

[10] M. Zecca et al., "Control of multifunctional prosthetic hands by processing the electromyographic signal," *Critical Rev. Biomed. Eng.*, vol. 30, no. 4-6, 2002.

[11] Ottobock, "Ottobock - global start," 2015. [Online]. Available: http://www.ottobock.com/

[12] V. T. Inman et al., "Relation of human electromyogram to muscular tension," *Electroencephalography and clinical neurophysiology*, vol. 4, no. 2, pp. 187–194, 1952.

[13] T. Moritani and H. A. DeVries, "Reexamination of the relationship between the surface integrated electromyogram (iemg) and force of isometric contraction." *American J. Physical Medicine & Rehabilitation*, vol. 57, no. 6, pp. 263–277, 1978.

[14] S. Metral and G. Cassar, "Relationship between force and integrated emg activity during voluntary isometric anisotonic contraction," *European J. applied physiology and occupational physiology*, vol. 46, no. 2, pp. 185–198, 1981.

[15] N. Hogan and R. W. Mann, "Myoelectric signal processing: Optimal estimation applied to electromyography-part i: Derivation of the optimal myoprocessor," *IEEE Trans. Biomed. Eng.*, vol. BME-27, no. 7, pp. 382–395, July 1980.

[16] ——, "Myoelectric signal processing: Optimal estimation applied to electromyography-part ii: experimental demonstration of optimal myoprocessor performance," *IEEE Trans. Biomed. Eng.*, vol. BME-27, no. 7, pp. 396–410, July 1980.

[17] E. A. Clancy and N. Hogan, "Probability density of the surface electromyogram and its relation to amplitude detectors," *IEEE Trans. Biomed. Eng.*, vol. 46, no. 6, pp. 730–739, June 1999.

[18] M. Harba and P. Lynn, "Optimizing the acquisition and processing of surface electromyographic signals," *J. biomed. eng.*, vol. 3, no. 2, pp. 100–106, 1981.

[19] A. Mannion and P. Dolan, "The effects of muscle length and force output on the emg power spectrum of the erector spinae," *J. Electromyography and Kinesiology*, vol. 6, no. 3, pp. 159–168, 1996.
[20] H. Milner-Brown and R. Stein, "The relation between the surface electromyogram and muscular force." *J. physiology*, vol. 246, no. 3, p. 549, 1975.
[21] J. Woods and B. Bigland-Ritchie, "Linear and non-linear surface emg/force relationships in human muscles: An anatomical/functional argument for the existence of both." *American J. Physical Medicine & Rehabilitation*, vol. 62, no. 6, pp. 287–299, 1983.
[22] J. H. Lawrence and C. De Luca, "Myoelectric signal versus force relationship in different human muscles," *J. Applied Physiology*, vol. 54, no. 6, pp. 1653–1659, 1983.
[23] C. M. Harris and D. M. Wolpert, "Signal-dependent noise determines motor planning," *Nature*, vol. 394, no. 6695, pp. 780–784, 1998.
[24] K. E. Jones et al., "Sources of signal-dependent noise during isometric force production," *J. neurophysiology*, vol. 88, no. 3, pp. 1533–1544, 2002.
[25] E. Todorov, "Cosine tuning minimizes motor errors," *Neural Computation*, vol. 14, no. 6, pp. 1233–1260, 2002.
[26] V. Witkovskỳ, "Computing the distribution of a linear combination of inverted gamma variables," *Kybernetika*, vol. 37, no. 1, pp. 79–90, 2001.
[27] D. A. Winter, *Biomechanics of human movement*. John Wiley & Sons Inc, 1979.
[28] T. Tsuji et al., "Impedance regulations in musculo-motor control system and the manipulation ability of the end-point," *Trans. of the Soc. of Instrument and Control Engineers*, vol. 24, no. 4, pp. 385–392, 1988, (in Japanese).

PLACE PHOTO HERE

Hideaki Hayashi (S'13–M'16) received the B.E., M.E., and D.Eng. degrees from Hiroshima University, Hiroshima, Japan, in 2012, 2014, and 2016, respectively. He is currently a Research Fellow of the Japan Society for the Promotion of Science (PD). His current research interests focus on machine learning, neural networks, and biological signal analysis.

PLACE PHOTO HERE

Akira Furui received the B.Eng degree from Hiroshima University, Hiroshima, Japan, in 2016. He is currently a master student in Graduate School of Engineering, Hiroshima University.

PLACE PHOTO HERE

Junichi Imagi received the B.E. and M.Eng degrees from Hiroshima University, Hiroshima, Japan, in 2013 and 2015, respectively.

PLACE PHOTO HERE

Yuichi Kurita (M'05) received a B.E. degree from Osaka University, Osaka, Japan in 2000, and M.E. and Ph.D. degrees in information science from Nara Institute of Science and Technology (NAIST), Nara, Japan in 2002 and 2004, respectively. Since 2011, he has joined the Institute of Engineering at Hiroshima University as an Associate Professor of the Biological Systems Engineering Laboratory. His research interests include cognitive physics, human biomechanics, haptics, and medical engineering.

PLACE PHOTO HERE

Toshio Tsuji (A'88–M'99) the B.E. degree in industrial engineering, and the M.E. and D.Eng. degrees in systems engineering from Hiroshima University, Hiroshima, Japan, in 1982, 1985, and 1989, respectively. He is currently a Professor in the Department of System Cybernetics, Hiroshima University. His current research interests focus on human-machine interface and computational neural sciences, in particular, biological motor control. Dr. Tsuji won the K. S. Fu Memorial Best Transactions Paper Award of the IEEE Robotics and Automation Society in 2003.